Seismic Amplification Within the Seattle Basin, Washington State: Insights from SHIPS Seismic Tomography Experiments

Catherine M. Snelson*, Thomas M. Brocher, Kate C. Miller, Thomas L. Pratt, and Anne M. Tréhu

*Previously at Department of Geological Sciences, University of Texas at El Paso, El Paso, TX 79968.

Abstract. Recent observations indicate that the Seattle sedimentary basin, underlying Seattle and other urban centers in the Puget Lowland, Washington, amplifies long period (1 to 5 s) weak ground motions by factors of 10 or more. We computed east-trending P- and S-wave velocity models across the Seattle basin from Seismic Hazard Investigations of Puget Sound (SHIPS) experiments in order to better characterize the seismic hazard the basin poses. The 3-D tomographic models, which resolve features to a depth of 10 km, for the first time define the P- and S-wave velocity structure of the eastern end of the basin. The basin, which contains sedimentary rocks of Eocene to Holocene age, is broadly symmetric in east-west section and reaches a maximum thickness of 6 km along our profile beneath north Seattle. A comparison of our velocity model with coincident amplification curves for weak ground motions produced by the 1999 Chi-Chi earthquake suggests that the distribution of Quaternary deposits, and reduced velocity gradients in the upper part of the basement east of Seattle, have significance in forecasting variations in seismic wave amplification across the basin. Specifically, eastward increases in the amplification of 0.2 to 5 Hz energy correlate to locally thicker unconsolidated deposits and a change from Crescent

Formation basement to pre-Tertiary Cascadia basement. Amplification curves at 7 to 9 s periods mirror the E-W symmetry of the basin. Seismicity within the Seattle basin along the profile lines up with this inferred basement contact and coincides with proposed strike-slip faults of Eocene age.

Introduction

The tectonic setting of the Pacific Northwest is dominated by oblique subduction of the Juan de Fuca plate beneath the North American plate (e.g., Riddihough, 1984; Monger and Nokleberg, 1996). This oblique plate convergence results in N-S shortening (Khazaradze *et al.*, 1999), such that both dextral strike-slip faults and east-trending thrust faults have formed in the Puget Lowland fore-arc basin (e.g., Johnson *et al.*, 1996; Pratt *et al.*, 1997; Wells *et al.*, 1998). Crustal faulting in the Puget Lowland has been accompanied by the formation of a series of thick, fault- or fold-bounded sedimentary basins beneath many of the urban centers in the region (Finn, 1990; Brocher *et al.*, 2001). Of these, the Seattle basin underlies the greatest population, including the cities of Seattle, Bremerton and Bellevue, Washington. The Seattle basin is also bounded to the south by the Seattle fault, which provides a source zone for potentially large earthquakes directly beneath these cities (Johnson *et al.*, 1994; Pratt *et al.*, 1997; Nelson *et al.*, 2003). Ominously, the Seattle basin also has been documented to substantially amplify long period seismic waves (e.g., Frankel *et al.*, 1999, 2002; Pratt *et al.*, 2003a, Barberopoulou *et al.*, 2004). In this paper, we use tomographic analyses of seismic data to examine the geometry and velocity structure of the Seattle basin and its influence on ground motions.

We use data from Seismic Hazard Investigations of Puget Sound (SHIPS) projects, a series of studies designed specifically to help characterize the seismic hazard in the region. There have been five SHIPS experiments to date: "Wet" SHIPS in 1998 (Fisher *et al.*, 2000); "Dry" SHIPS in

1999 (Brocher *et al.*, 2000a, 2000b); "Kingdome" SHIPS in 2000 (Brocher *et al.*, 2000a, 2002); "Seattle" SHIPS in 2002 (Pratt *et al.*, 2003b); and "Bellingham" SHIPS in 2002 (Brocher *et al.*, 2003). The 1999 and 2000 experiments were designed to study the Seattle basin, and it is those data we analyze here. We conducted the "Dry" SHIPS experiment (Figure 1) in September 1999 to better define the E-W geometry of the Seattle basin and to determine the velocity structure of the Cenozoic sedimentary basin fill. The March, 2000 SHIPS experiment recorded data during the Kingdome sports arena implosion in downtown Seattle, as well as four small blasts (Figure 1) ("Kingdome" SHIPS).

In this paper, we present results of our tomographic analysis of data acquired during "Dry" and "Kingdome" SHIPS. The results provide the first detailed P- and S-wave velocity models across the Seattle basin in an east-west direction, giving insights into the tectonic evolution of the Seattle basin and its influence on ground shaking.

Geologic Background

During early Paleogene time (~50 Ma), Paleocene to mid-Eocene age basaltic and sedimentary rocks of the Crescent Formation (Siletz volcanic terrane) were accreted to western North America (Tabor and Cady, 1978; Johnson *et al.*, 1984, 1985; Atwater, 1989; Burchfiel *et al.*, 1992). The Crescent Formation now forms the basement rocks of western Washington State, including the Puget Lowland, and acts as a backstop for the accumulation of the accretionary wedge (e.g., Tabor and Cady, 1978; Atwater, 1989; Brandon and Calderwood, 1990; Brandon and Vance, 1992). Crescent Formation rocks underlying the western side of the Puget Lowland are in contact with pre-Tertiary Cascade volcanic rocks beneath the eastern side of the Lowland (Tabor and Cady, 1978; Johnson, 1984, 1985; Atwater, 1989). The location of this basement contact is not

well defined, but the velocity and density contrast between the basement rocks likely influences basin geometry and potential seismic wave amplification (e.g., Finn, 1990; Pratt *et al.*, 2003a).

Crescent Formation basement rocks are compressed in a series of folds and faults that form uplifted blocks and down dropped basins beneath the Puget Lowland. The most prominent of these uplifted blocks, the Seattle uplift, lies immediately south of the Seattle basin and is bounded by the Seattle and Tacoma fault zones (Pratt *et al.*, 1997; Brocher *et al.*, 2001, 2004; Johnson *et al.*, 2004; Sherrod *et al.*, 2004). Recently, simultaneous inversions of gravity data and tomography models from the 1998 SHIPS experiment have refined the sub-surface picture of the Seattle fault and Seattle basin (Brocher *et al.*, 2001; Parsons *et al.*, 2001; ten Brink et al., 2002).

The stratigraphy within the Seattle basin is known from surface exposures, industry boreholes, and seismic reflection profiles tied to the boreholes (Figure 1c; Johnson *et al.*, 1994, 1999; Brocher and Ruebel, 1998; Rau and Johnson, 1999). As much as 1.1 km of unconsolidated, primarily Quaternary and Holocene deposits (Jones, 1996) form the top of the basin and are thought to be the main contributor to the amplification of seismic energy (Frankel *et al.*, 1999, 2002; Pratt *et al.*, 2003a; Barberopoulou *et al.*, 2004). The upper portions of the unconsolidated deposits are a temporally and spatially complex stratigraphy of glacial outwash, till, lacustrine, and recessional deposits formed when the Lowland was glaciated at least six different times in the Pleistocene (Booth, 1994). Well logs and seismic reflection data indicate that these Quaternary and Holocene deposits overlie sedimentary rocks of Eocene to Miocene age (Figure 1c).

The Seattle fault zone bounds the Seattle basin to the south, and consists of several east-west trending faults (Johnson *et al.*, 1999; Blakely *et al.*, 2002). Motion on the Seattle fault has caused a north-south asymmetry to the Seattle basin, wherein the basin thins from 7 to 10 km near the fault to about 2.5 km at its northern end (Johnson *et al.*, 1994; Pratt *et al.*, 1997; Brocher *et al.*,

2001, 2004; ten Brink *et al.*, 2002; Van Wagoner *et al.*, 2002). The western end of the Seattle fault zone is thought to lie at the east edge of the Olympic Mountains, whereas the eastern end of the fault is interpreted to lie near the base of the Cascade Range near the southeast projection of the Southern Whidbey Island fault (Gower *et al.*, 1985; Finn, 1990; Johnson *et al.*, 1994, 1996; Pratt *et al.*, 1997; Brocher *et al.*, 2001).

Several large crustal earthquakes ruptured the Puget Lowland during the late Holocene (Bucknam *et al.*, 1992; Haugerud *et al.*, 2003; Nelson *et al.*, 2003; Sherrod *et al.*, 2004). The best documented of these occurred about 1000 to 1100 years ago on the Seattle fault, causing 7 m of uplift, fault scarps, a tsunami, and landslides (Bucknam *et al.*, 1992; Atwater and Moore, 1992; Nelson *et al.*, 2003; Schuster *et al.*, 1992). This evidence suggests that the Seattle fault zone can produce M 7.0+ earthquakes (Bucknam *et al.*, 1992; Pratt *et al.*, 1997).

Data Acquisition and Analysis

Acquisition. The 1999 SHIPS seismic refraction line crossed the Seattle basin in an east-west direction. The profile was ~ 117 km in length, and extended from the Olympic Mountains, through north Seattle, to the foothills of the Cascades (Figure 1b). Four shorter and less densely instrumented cross lines provide constraints on the shallow, three-dimensional structure of the eastern side of the basin.

During the 1999 SHIPS experiment (Brocher *et al.*, 2000a), 1008 seismometers were installed along the lines with a nominal spacing of 100 m. To record shear waves, 239 of our instruments were 3-component recorders distributed nominaly at 400 m spacing. For sources, we detonated 38 shots at 29 sites, with a nominal spacing of 4 km and charge sizes ranging from 11 to 1136 kg. Overall the data quality was good to high (Figure 2).

The March 2000 "Kingdome SHIPS" experiment was designed to study the site response and the velocity structure within the upper 2 km of the Seattle basin (Brocher *et al.*, 2000b, 2002). We deployed a hexagonal grid of 206 seismic recorders within the city of Seattle (box in Figure 1b), with a nominal station spacing of about 1 km. In addition to recording the implosion of the Kingdome sports arena for site response analysis, we detonated four 68-kg shots at the corners of the grid for shallow tomographic analysis.

Analysis. We derived velocity models from the combined 1999 and 2000 SHIPS data using the 3-D tomographic method of Hole (1992). Important parameters included the choice to implement the code in 3-D, the starting 1-D velocity model, and the smoothing schedule for updating velocity models. We chose a 3-D approach because of the crooked-line geometry of the 1999 SHIPS profile (Figure 1). Our 3-D model space was 137 km in length (E-W) by 51 km wide (N-S) and 40 km deep with a 400 m grid spacing (dashed line in Figure 1b). We present 2-D velocity models and hit counts (number of rays/cell) derived from our 3-D grid. The 2-D velocity models collapse the 3D grid by weighting model values by the hit count, and then summing in the north-south direction.

The initial 3-D, P-wave model was an expansion of a 1-D velocity model compiled from *a priori* information for the study area (e.g., Parsons *et al.*, 1999; Hiett, 2000). We derived our final P-wave model from the inversion of over 13,000 P-wave first-arrival traveltime picks. We estimate the traveltime picking error for the first arrivals to be ~ 0.1 s in high signal-to-noise ratio portions of the seismic data, and is ~ 0.15 s otherwise. Our starting model produced a RMS (root mean square) error of 1.34 sec. We carried out 3 runs of ten iterations each to produce the final model. The first and second runs used a smoothing factor of 40 x 40 x 20 grid nodes (16 km x 16 km x 8 km) and 30 x 30 x 10 grid nodes (12 km x 12 km x 4 km) respectively. The final run used a

smoothing factor of 20 x 20 x 10 grid nodes (8 km x 8 km x 4 km) and produced a model with an RMS error equal to the estimated picking error of ~ 0.1 s. A detailed examination of the fit between observed and calculated travel times shows that there are places where the misfit is much less than 0.1 s as well as places where it is as large as 0.2 s (Figure 3a).

Times for over 1500 arrivals were inverted for the S-wave velocity model. The quality of the S-wave arrivals on the horizontal component data is fair to good, and several of the 1999 shots produced obvious shear wave arrivals across the entire length of the profile. Many shots recorded on the horizontal components are highly reverberatory, which made picking the S-wave arrivals difficult. To address this problem, the P-wave first arrival times were converted to approximate S-wave arrival times assuming a Poisson's ration of 1.8 and then used as a guide for picking S-wave arrivals. This approach worked as a first order approximation. The initial S-wave velocity model was converted from the final P-wave model using a Vp/Vs ratio of 1.8, which is appropriate for basement rocks in the study area (Brocher and Christensen, 2001). The S-wave arrivals were then inverted using the 3-D approach described by Hole (1992). The initial S-wave model had a 1-km grid cell spacing. The final RMS error for the S-wave model is 0.2 s, which is comparable to our estimate of the picking error for these arrivals (Figure 3b).

A sense of the spatial resolution of the P- and S-wave velocity models can be obtained by jointly examining the RMS error, travel time fits, hit count, and checkerboard tests. Unfortunately, the non-linear technique we used does not produce a resolution matrix (Hole, 1992). The number of rays that intersect (hit) any given cell provides an estimate of the resolution in that cell. Overall, the ray coverage is adequate throughout the P-wave model, with a minimum of 5 hits and a maximum of 1884 hits per cell, whereas the hit count for the S-wave model reaches a maximum 420 hits per cell (Figure 4). The ray coverage is especially dense where shots were fired twice at

the same location. Ray coverage from the 1999 SHIPS cross lines and 2000 SHIPS data was adequate in the upper 2 km, but decreased rapidly below that depth (Snelson, 2001). Because the southwest corner shot in the 2000 SHIPS experiment was not well recorded, the southern portion of the grid, which crossed the Seattle fault, provides limited ray coverage. The maximum depth of ray penetration is 16 km for the P-wave model and 24 km for the S-wave model.

Following the resolution test method of Zelt (1998), 2D checkerboards with 15 km x 15 km, 10 km x 10 km, and 5 km x 5 km sinusoidal checkers with amplitudes of ±3% were added to a smoothed 1-D version of the final P-wave velocity model. Traveltimes from this model were calculated to serve as "observed" traveltimes in an inversion run that smoothed 1-D model as input. The inversion was then allowed to run for five iterations. The shapes of the checkers above 7 km depth were well recovered with the 15 km checkers, and those above 4 km depth were recovered with 10 km checkers We could not adequately recover the 5 km checkers (Figure 5). These results suggest that the best resolution is in the upper 7 km of the model (Figure 5), which sufficient for imaging the base of the Seattle basin.

Results

Seattle Basin Geometry. Our tomography results show that in east-west profile, the Seattle basin is a nearly symmetric, bowl-shaped region of low-velocity (1.7 - 4.5 km/s) rocks and sediments with sides sloping about 20º on the east and 29º on the west (Figure 6). As explained below, we interpret the bottom of the sedimentary basin to be at or near the 4.5 km/s contour on the P-wave velocity model. The length of the Seattle basin on our profile is ~76 km measured from where the 4.5 km/s contour comes within 1 km of the surface at each end (Figure 6). The maximum basin thickness along our profile is about 6 km, which is consistent with the profile's location several km to the

north of the thickest (~7 to 10 km thick) part of the basin as interpreted from north-south trending seismic reflection profiles (Johnson *et al.*, 1994; ten Brink *et al.*, 2002), gravity, and 3D tomographic models (Brocher et al., 2001; Van Wagoner *et al.*, 2002). The eastern edge of the basin lies near the interpreted southeast projection of the Southern Whidbey Island fault (Johnson *et al.*, 1996). The western edge lies near the hypothesized Hood Canal-Discovery Bay fault (Gower *et al.*, 1985; Johnson *et al.*, 1994). Neither end of the basin shows an abrupt step consistent with significant displacement by a fault, although a small (<0.5 km) step would be below the resolution of our model.

Our profile ties the north-trending, 1998 SHIPS seismic reflection line at model km 62 at Puget Sound (Figure 6; ten Brink *et al.*, 2002), which is in turn tied to the Mobil-Kingston #1 well (Figure 7). In the Kingston well, the top of Crescent Formation is interpreted as basalt interbedded with siltstone, tuff, and conglomerate (Rau and Johnson, 1999), and these rocks correspond to the depth where seismic velocities reach 4.5 km/s (ten Brink *et al.*, 2002). We therefore use the 4.5 km/s velocity contour as a proxy for the top of the Crescent Formation and the bottom of the Seattle basin.

The maximum basin thickness in our model is close to that determined by ten Brink et al. (2002) and is similar to that inferred from the north-trending 1991 Washington refraction line intersecting our profile at model km 94 (Figures 1a and 7; Miller *et al.*, 1997). The combination of our results and the N-S profiles confirm that the basin is asymmetric in the north-south direction but nearly symmetric in the east-west direction (Johnson *et al.*, 1994; Pratt *et al.*, 1997; Brocher *et al.*, 2001; ten Brink *et al.*, 2002).

The asymmetry of the Seattle basin in a north-south direction has been inferred to be the result of its formation in response to motion on the Seattle fault zone (Johnson *et al.*, 1994).

Consistent with this hypothesis, documented uplift above the Seattle fault during Holocene earthquakes reaches a maximum near the center of the basin (Bainbridge Island), where high resolution topography (Light Detection and Ranging, or LIDAR) have revealed the best evidence for surface faulting along the Toe Jam scarp (Nelson *et al.*, 2003). If the basin shape is indeed caused by the motion on the Seattle fault, the ~76 km width of the basin on our profile implies the Seattle fault is at least that length. The Seattle fault may be a few km longer than the basin width imaged on our profile because our profile is located about 5 km north of the Seattle fault zone and the width of the basin decreases northward (Brocher *et al.*, 2001, 2004).

Unconsolidated deposits in the Seattle basin. Unconsolidated deposits that are primarily Holocene and Quaternary age, but that include older units, are defined on our profile based on their relatively low velocities (Figure 6). ten Brink *et al.'s* (2002) correlation with the Mobil-Kingston #1 well found that Quaternary and older unconsolidated units have velocities less than 2.5 km/s. This correlation is also compatible with borehole logs (Figure 7). The average velocity of Pleistocene units in these well logs is 1.6 to 1.8 km/s, but older unconsolidated deposits have velocities up to 2.4 km/s.

Assuming that the 2.5 km/s velocity contour represents the base of the unconsolidated deposits in our model, their thickness within the Seattle basin reaches up to 1 km along our profile (Figure 6a). Our estimated 1 km depth to the base of unconsolidated deposits in Puget Sound matches those of ten Brink *et al.* (2002) and Calvert *et al.* (2003), based on seismic reflection profiles along the SHIPS 98 transect and high-resolution seismic tomography. Our estimated thickness is ~ 2 times greater than that inferred solely from high-resolution seismic reflection data

(Frankel and Stephenson, 2000), and is thicker than that inferred by Jones (1996) from drill holes on nearby land and industry seismic reflection data.

Shallow sub-basins within the Seattle basin. Tomographic analysis of the 1998 Wet SHIPS traveltimes suggest the Seattle basin has several sub-basins defined by closed velocity contours in map view (Brocher *et al.*, 2001). In cross section, there is evidence from our model for up to three sub-basins, based on thickness variations of the unconsolidated deposits (Figure 6b). Between Hood Canal and Puget Sound (beneath the Kitsap Peninsula) we identify a well-defined depression in the 2.5 km/s contour that we label as Sub-basin 1. Between Puget Sound and model km 92, (beneath Seattle and Redmond) there is another well-defined depression that we call Sub-basin 2. Between model km 92 and 100, near Lake Sammamish, we identify another, smaller depression that we label Sub-basin 3. A region of higher velocity material beneath Puget Sound separates sub-basins 1 and 2, and suggests that the base of the unconsolidated deposits may also shoal. Because ground motions are dependent on the velocities within the shallow deposits, these sub-basins may yield variations in ground motions during earthquakes (discussed below).

Tertiary Sedimentary Rocks in the Seattle basin. In our tomography model, Eocene to Miocene sedimentary rocks have velocities between 2.5 and 4.5 km/s. At km 62, where our model intersects the 1998 SHIPS seismic reflection line (ten Brink *et al.*, 2002), the 3.8 km/s velocity contour corresponds approximately to the interpreted bottom of the Oligocene Blakeley Formation. At this location velocities of less than 2.8 km/s correspond approximately to interpreted Miocene Blakely Harbor Formation (Figure 6), making this formation relatively thin on our profile. These estimates of P-wave velocities are close to those inferred from sonic logs (Figure 7), which show velocities

for the Oligocene Blakeley Formation to vary between 2.4 and 3.6 km/s and Eocene sedimentary rocks to have velocities between 2.8 and 4.0 km/s (Figure 7).

Location of the Crescent/Cascadia Basement Contact. In the upper part of the basement rocks, at model km 70 near Seattle, we identify a pronounced, eastward decrease in the vertical velocity gradient at a depth of 6 km that we interpret as the change from Crescent Formation to pre-Tertiary Cascade basement rocks (Figure 6). This decreased velocity gradient, which our checkerboard test suggests is well resolved, was also reported by Van Wagoner *et al.* (2002) on a nearby cross section parallel to ours, and is consistent with lower velocities within the pre-Tertiary Cascade basement rocks compared to the Crescent Formation (Miller *et al.*, 1997). An east-trending refraction profile near ~46.5˚E indicates that the Crescent/Cascade basement contact at the Mt. St. Helens seismic zone (SHZ, Figure 1) is represented by a sharp eastward decrease in basement velocity (Parsons *et al.*, 1999). The contact is more subtle along our profile.

Our proposed location for the Crescent/Cascade basement contact near model km 70 coincides with postulated north-trending strike-slip faults of Eocene age (Figure 8; Johnson, 1984, 1985; Johnson *et al.*, 1999) and with a vertical band of seismicity in the upper 5 km of the Seattle basin (Figure 1a and 9),. The seismicity represents a couple of earthquake swarms rather than a long-term seismic zone, but could indicate a basement fault extending into the sedimentary strata.

P-wave velocities increase with depth in the model, reaching a maximum of ~7.2 km/s at 11 km depth. Velocities this high probably correspond to mafic members of the Crescent Formation volcanic rocks (Brocher and Christensen, 2001). An isolated high velocity anomaly (>6.5 km/s) on the west side of the model, just east of Hood Canal at a depth of 5 to 8 km, also may represent a more mafic component of the Crescent Formation (Figure 6). However, the checkerboards tests

reveal that below 7 km the model is not well resolved, and therefore the velocities at the base of the model may not be accurate.

S-wave velocity model for the Seattle basin. As expected, the general features of our S-wave velocity model are similar to those of our P-wave model**.** These similarities include the overall shape of the Seattle basin, the existence of shallow sub-basins, and a high-velocity body near Hood Canal.

Our study provides the first detailed S-wave velocity model for the Seattle basin. Our model shows S-wave velocities for Cenozoic sedimentary rocks within the basin ranging from 1 km/s up to 2.6 km/s (Figure 9). Near-surface S-wave velocities within the basin are less than 1 km/s in the west end of the basin (sub-basin 1) increase to 1.3 km/s in the center of the basin (Sub-basin 2), and decrease in the eastern end of the basin to 1.1 km/s (sub-basin 3; Figure 9). The very near-surface velocities are consistent with recent shallow seismic measurements (e.g., Odum et al., 2004). S-wave velocities for the Miocene Blakely Harbor Formation range up to 1.7 km/s, for the Oligocene Blakeley Formation S-wave velocities vary from 1.7 to 2.0 km/s, and for the Eocene sedimentary rocks S-wave velocities range from 2.0 to 2.6 km/s (Figure 9). S-wave velocities at the base of the Cenozoic sedimentary rocks filling the basin are close to 2.6 km/s, corresponding to a Vp/Vs of 1.73 for the deep sedimentary strata.

S-wave velocities in the Crescent Formation volcanic basement rocks are substantially higher than those in the basin (Figure 9). Along the Olympic Peninsula, where Crescent Formation rocks crop out, S-wave velocities exceed 2 km/s, even at the surface. Where the Crescent Formation is overlain by a substantial sedimentary cover, our model indicates S-wave velocities near 2.6 km/s at the top of the Crescent Formation, increasing to velocities of about 3.5 km/s at

depths of about 10 km, and to 4 km/s at depths of 15 km at the center of the model. These velocities approximate the average Vs observed in the laboratory for 29 different samples of the Crescent Formation (Brocher and Christensen, 2001). Our P- and S-wave models yield Vp/Vs ratios of 1.71 to 1.81 for the Crescent Formation at depth, consistent with laboratory measurements of Vp/Vs (Brocher and Christensen, 2001).

Implications for Seismic Hazard and Crustal Structure

Comparison of Seattle Basin Geometry to Weak Ground Motions. Urban sedimentary basins, including the Seattle basin, represent a significant seismic hazard due to their tendency to amplify ground motions (Frankel *et al.*, 1999, 2002; Pratt *et al.*, 2003a; Barberopoulou *et al.*, 2004). Sedimentary basins beneath Los Angeles, Mexico City, and elsewhere amplify ground motions at the resonance period of the basins (Jongmans *et al.*, 1998; Wald and Graves, 1998). Amplification of strong ground motions around the edges of basins has been interpreted as resulting from interference patterns along crustal fault zones and thinning basins (Kawase, 1996; Graves *et al.*, 1998). Finally, surface waves generated within these basins are thought to be responsible for much of the increased amplitude and duration of shaking during earthquakes (Frankel *et al.*, 1999, 2002; Pratt *et al.*, 2003a; Barberopoulou *et al.*, 2004). A detailed understanding of basin geometry is critical for understanding and forecasting these phenomena (e.g., Frankel and Stephenson, 2000; Pitarka et al., 2004). Our velocity models better characterize the Seattle basin geometry, and therefore can be used to better assess the variations in ground motion expected for the basin.

As discussed earlier, the Seattle basin contains up to three shallow sub-basins defined by local increases in the thickness of unconsolidated deposits (Figure 6b and 10b). Given the low

shear- and compressional-wave velocities in these sub-basins, their spatial distribution has importance for predicting lateral variations in site response.

Observations of weak ground motions in the Seattle basin during the 1999 SHIPS experiment indicate an amplification of the long period motions (3 to 5 s periods) by a factor or 10 or more relative to bedrock sites in the Olympic Peninsula (Figure 9a) (Pratt *et al.*, 2003a). All frequencies below about 7 Hz show amplification, with the peak being about 0.33 Hz (3 s periods). These observations were made using arrivals from the 1999 Chi-Chi, Taiwan earthquake, local earthquakes and blasts recorded on a subset of our SHIPS seismometers, and therefore are coincident with the velocity models shown in Figure 6b and 10. We plot these amplification curves over the S-wave velocity model in Figure 9 to facilitate comparison of basin structure with amplification (Figure 9a).

The primary observation is that at periods of 1 to 7 s the amplification curves are not symmetric across the basin but are skewed, with the largest amplifications occurring over the east-central part of the basin (near Lake Washington). From this asymmetry, we infer that the general basin geometry and overall thickness of Cenozoic sedimentary rocks is not the primary factor in controlling the observed weak-ground motion amplification for periods of more than 1 s. Instead, we note that the largest amplifications coincide with the thickest section of unconsolidated deposits, in sub-basin 2, near Lake Washington (Figure 9a). Pratt *et al.* (2003a) attributed most of the amplification to resonance in the shallow strata and to the generation of surface waves, both of which may correlate with the thickness and low velocity of unconsolidated deposits. These results thus are consistent with Pratt *et al.*'s (2003a) conclusion that the unconsolidated deposits largely control the amplification.

The largest amplifications lie east of the inferred Crescent/Cascadia basement contact at model km 70, above the pre-Tertiary Cascadia basement (Figure 9). Hence, another possible contributor for this asymmetrical amplification is focusing by the Cascadia basement rocks (Pratt *et al.,* 2003a). Pratt *et al.* (2003a) performed ray tracing through the P-wave velocity model shown in Figure 6b (the S-wave model was not yet available) and suggested that the overall basin geometry would lead to only 5 to 10% amplification of the arrivals. However, our S-wave velocity model shows a decrease in the velocities in the 10 to 15 km depth range beneath sub-basin 2, and this deep, low-velocity zone could focus S-wave energy into sub-basin 2. Specifically, the S-wave arrivals from the Chi-Chi earthquake, which came from the west, could be refracted at the interface between the basement rocks, focusing energy toward the east side of the basin. Thus, it may be that a combination of thicker, slower near-surface deposits and focusing from deeper velocity anomalies cause the largest amplifications to occur in the east-central portion of the Seattle basin.

Pratt *et al.* (2003a) noted that at higher frequencies, at 7 Hz and above, intrinsic attenuation within the basin may damp out seismic energy and cause de-amplification. This inference is supported by recent estimates of high intrinsic attenuation within the Seattle basin (Pratt and Brocher, 2004; Li *et al.*, 2004).

Finally, amplification curves for the 1999 Chi Chi earthquake for periods between 7 and 9 seconds exhibit greater symmetry and less amplification than for periods between 3 and 7 seconds (Figure 9). This greater symmetry of the long-period amplification mirrors the overall symmetry of the basin. Thus, we infer that at these long periods the overall basin geometry exerts an influence on the amplifications.

Other Seismic Hazard Implications

As described earlier, the Seattle basin may have formed in response to motion on the Seattle fault, in which case the basin shape may be a proxy for the slip distribution of earthquakes on the Seattle fault (Johnson *et al.*, 1994; ten Brink *et al.*, 2002). This notion is supported by the fact that the thickest part of the basin, near Seattle, coincides with the best-developed Holocene fault scarps (Nelson *et al.*, 2003) and the largest land-level uplifts (Bucknam et al., 1992). Our observation that the basin is at least 76 km long implies a fault of this length, and a maximum magnitude of 7.2 for earthquakes on the fault zone assuming a down-dip extent of 20 km (Wells and Coppersmith, 1994).

The presence of shallow sub-basins in the Seattle basin, with the boundary between the two major sub-basins coinciding with hypothesized N-S faults and a change in location of the surface expression of the Seattle fault (Johnson *et al.*, 1999; Blakely *et al.*, 2002), raises the possibility that at least the uppermost parts of the Seattle fault zone are segmented. Brocher *et al.* (2004) interpret the Seattle fault zone as a passive roof duplex, with a north-vergent triangle zone bounded above by a shallow roof thrust. Segmentation of the roof thrusting may explain our observations of sub-basins, and we note that such segmentation does not require segmentation of the master floor thrust inferred by Brocher *et al.* (2004).

Crescent Terrane/Cascadia basement contact

Interpretations of seismic refraction profiles in the Cascades (Miller *et al.*, 1997) and near Mount Saint Helens (Parsons *et al.*, 1999), suggest that reduced velocity gradients in the upper part of the basement rocks near Seattle (km 70 of the model) mark the contact between the Crescent Formation and pre-Tertiary Cascade basement rocks. To the north of the Seattle basin, the Southern Whidbey Island fault has been proposed to form this contact (Johnson *et al.*, 1996), and Blakely *et*

al. (2004) summarized evidence for aeromagnetic and LIDAR topographic lineations along the SE projection of the Southern Whidbey Island fault to the north of our transect. Placing the contact between the Crescent Formation and pre-Tertiary Cascade basement rocks at km 70 of the model would require either a sharp southerly bend in any possible SE extension of the Southern Whidbey Island fault not observed in the aeromagnetic lineations (Blakely *et al.*, 2004), or would require the contact to have formed along a different fault in this location (Johnson, 1984, 1985). Seismicity along the profile better supports the latter interpretation as it lines up with the lower velocity gradient near Seattle and coincides at the surface with the location of a proposed N-trending strike-slip fault (Figure 6) (Johnson *et al.*, 1994, 1999).

Tectonic Implications

The mild asymmetry of the Seattle basin, with a western end that dips more steeply than the eastern end, could have resulted from uplift of the Olympic Mountains in response to growth of the accretionary wedge (Brandon and Calderwood 1990; Brandon and Vance, 1992). Uplift would have been produced by underthrusting of the Olympic core complex beneath the Crescent Formation, that resulted in flexure of the Crescent Formation on the west side of the Puget Lowland (Crosson and Symons, 2001). The west edge of the basin may therefore be controlled by a combination of motion on the Seattle fault and flexure caused by the underthrusting. Flexure of the Crescent Formation locally may, in part, be responsible for diffuse crustal seismicity at 20 to 30 km depth beneath Puget Lowland, but the overriding N-S compression is due to oblique nature of the subduction (e.g., Van Wagoner *et al.*, 2002).

Acknowledgements

This work was supported by the USGS Urban Geological Hazards Initiative, and external grants from the USGS National Earthquake Hazards Reduction Program to Oregon State University, the University of Texas El Paso, and the University of Washington. The instruments used in the field program were provided by the Geological Survey of Canada and the PASSCAL facility of the Incorporated Research Institutions for Seismology (IRIS) through the PASSCAL Instrument Center at New Mexico Tech. Data collected during this experiment will be available through the IRIS Data Management Center. The facilities of the IRIS Consortium are supported by the National Science Foundation under Cooperative Agreement EAR-0004370. We thank the Washington State Departments of Forestry and Parks and Recreation, Olympic National Forest, the Bureau of Land Management, Kitsap and King Counties, and the Cities of Bainbridge Island, Seattle, and Redmond for permission to access land under their jurisdiction. We thank the Weyerhaeuser Corp., International Paper Co., and numerous property owners for permission to access their land. Tom Burdette, USGS, organized and arranged permits for the fieldwork. We thank all those who helped to survey the lines, deploy and retrieve the recorders, and load and detonate the shots. We would like to thank Shirley A. Baher, Aggeliki Barberopoulou, and Brett T. McLaurin for their early reviews of this paper.

References

Atwater, T. (1989). Plate tectonic history of the northeast Pacific and western North America, in *The Eastern Pacific Ocean and Hawaii*, E. L. Winterer, D. M. Hussong, and R. W. Decker (Eds.), Geological Society of America, The Geology of North America, **N**, 21-72.

Atwater, B. F., and A. L. Moore (1992). A tsunami about 1000 years ago in Puget Sound, Washington, *Science* **258**, 1614-1617.

Barberopoulou, A., A. Qamar, T. L. Pratt, K. C. Creager, and W. P. Steele (2004). Local amplification of seismic waves from the Denali earthquake and damaging seiches in Lake Union, Seattle, Washington, *Geophys. Res. Lett.* **31**, L03607, doi 10.1029/2003GL018569.

Blakely, R. J., R. E. Wells, C. S. Weaver, and S. Y. Johnson (2002). Location, structure, and seismicity of the Seattle fault, Washington: Evidence from aeromagnetic anomalies, geologic mapping, and seismic-reflection data, *Geol. Soc. Am. Bull.* **114**, 169-177.

Blakely, R. J., B. L. Sherrod, R. E. Wells, C. S. Weaver, D. H. McCormack, K. G. Troost, and R. A. Haugerud (2004). The Cottage Lake Aeromagnetic Lineament: A possible onshore extension of the southern Whidbey Island fault, Washington, *U.S. Geol. Surv. Open-File Rept. 2004-1204,* 61 p. http://pubs.usgs.gov/of/2004/1204.

Booth, D. B. (1994). Glaciofluvial infilling and scour of the Puget Lowland, Washington, during ice-sheet glaciation, *Geology* **22**, 695-698.

Brandon, M. T., and A. R. Calderwood (1990). High-pressure metamorphism and uplift of the Olympic subduction complex, *Geology* **18**, 1252-1255.

Brandon, M. T., and J. A. Vance (1992). Tectonic evolution of the Cenozoic Olympic subduction complex, Washington State, as deduced from fission track ages for detrital Zircons, *Am. J. Science* **292**, 565-636.

Brocher, T. M., and A. L. Ruebel (1998). Compilation of 29 sonic and density logs from 23 oil test wells in western Washington State, *U.S. Geol. Surv. Open-File Rept. 98-249*, 41 pp.

Brocher, T. M., and N. I. Christensen (2001). Density and velocity relationships for digital sonic and density logs from coastal Washington and laboratory measurements of Olympic Peninsula mafic rocks and greywackes, *U.S. Geol. Surv. Open-File Rept.* **01-264**, 39 pp.

Brocher, T. M., and K. Ramachandran (2004). Relationships between upper crustal structure in the Cascadia Forearc and Juan de Fuca-North America plate convergence, Washington State and British Columbia, *Geophy. Res. Lett*., in prep.

Brocher, T. M., K. C. Miller, A. M. Tréhu, C. M. Snelson, T. L. Pratt, C. S. Weaver, K. C. Creager, R. S. Crosson, U. S. ten Brink, M. G. Alvarez, S. H. Harder, and I. Asudeh (2000a). Report for explosion and earthquake data acquired in the 1999 Seismic Hazards Investigation of Puget Sound (SHIPS), Washington, *U.S. Geol. Surv. Open-File Rept.* **2000-318**, 85 pp. http://geopubs.wr.usgs.gov/open-file/of00-318/.

Brocher, T. M., T. L. Pratt, K. C. Creager, R. S. Crosson, W. P. Steele, C. S. Weaver, A. D. Frankel, A. M. Tréhu, C. M. Snelson, K. C. Miller, S. H. Harder, and U. S. ten Brink (2000b). Urban seismic experiments investigate Seattle fault and basin, *Eos, Trans. Am. Geophys. Un.* **81**, 545, 551-552.

Brocher, T. M., T. Parsons, R. A. Blakely, N. I. Christensen, M. A. Fisher, R. E. Wells, and the SHIPS Working Group (2001). Upper crustal structure in Puget Lowland, Washington: Results from 1998 Seismic Hazards Investigation in Puget Sound, *J. Geophy. Res*. **106,** 13,541-13,564.

Brocher, T. M., T. L. Pratt, C. S. Weaver, C. M. Snelson, and A. D. Frankel (2002). Seismic recordings from the 2000 Kingdome Seismic Hazards Investigation in Puget Sound (SHIPS), Washington, *U.S. Geol. Surv. Open-File Rept.* **02-123**, 29 pp. http://geopubs.wr.usgs.gov/open-file/of02-123/.

Brocher, T. M., T. L. Pratt, G. D. Spence, M. Riedel, and R. D. Hyndman (2003). Wide-angle seismic recordings from the 2002 Georgia Basin Geohazards Initiative, Northwestern Washington and British Columbia, *U.S. Geol. Surv. Open-File Rept.* **03-160**, 34 pp. http://geopubs.wr.usgs.gov/open-file/of03-160/.

Brocher, T. M., R .J. Blakely, and R. E. Wells (2004). Interpretation of the Seattle uplift, Washington, as a passive roof duplex, *Bull. Seism. Soc. Am*., **94**, 1379-1401.

Bucknam, R. C., E. Hemphill-Haley, and E. B. Leopold (1992). Abrupt uplift within the past 1700 years at southern Puget Sound, Washington, *Science* **258**, 1611-1614.

Burchfiel, B. C., D. S. Cowan, and G. A. Davis (1992). Tectonic overview of the Cordilleran orogen in the western United States, in *The Cordilleran Orogen: Conterminous U.S.*, B. C. Burchfiel, P.W. Lipman, and M. L. Zoback (Eds.), Geological Society of America, The Geology of North America, **G-3**, 407-479.

Calvert, A. J., M. A. Fisher, S. Y. Johnson, T. M. Brocher, K. C. Creager, R. S. Crosson, R. D. Hyndman, K. C. Miller, D. Mosher, T. Parsons, T. L. Pratt, G. Spence, U. ten Brink, A. M. Trehu and C. S. Weaver (2003). Along-strike variations in the shallow seismic velocity structure of the Seattle fault zone; evidence for fault segmentation beneath Puget Sound, *J. Geophys. Res*. **108**, doi 10.1029/2001JB001703, 14 pp.

Crosson, R. S. and N. P. Symons (2001). Flexural origin of the Puget basins: Implications for the Seattle fault and Puget basin tectonics (abstract). *Eos, Trans., AGU* **82**(47): F856.

Danes, Z. F., M. M. Bonno, E. Brau, W. D. Gilham, T. F. Hoffman, D. Johansen, M. H. Jones, B. Malfait, J. Masten, and G. O. Teague (1965). Geophysical investigation of the southern Puget Sound area, Washington, *J. Geophys. Res*. **70**, 5573-5580.

Finn, C. (1990). Geophysical constraints on Washington convergent margin structure, *J. Geophys. Res*. **95**, 19,533-19,546.

Fisher, M. A., A. J. Calvert, T. Parsons, R. E. Wells, T. M. Brocher, C. S. Weaver, and the SHIPS Working Group (2000). Crustal structure from SHIPS seismic reflection data along a transect from the southern Puget Lowland north to the San Juan Islands, *Eos, Trans. Am. Geophys. Un*.

81, 878.

Frankel, A., and W. Stephenson (2000). Three-dimensional simulations of ground motions in the Seattle region for earthquakes in the Seattle fault zone, *Bull. Seism. Soc. Am.* **85**, 1251-1267.

Frankel, A., D. Carver, E. Cranswick, M. Meremonte, T. Bice, and D. Overturf (1999). Site response for Seattle and source parameters of earthquakes in the Puget Sound region, *Bull. Seism. Soc. Am.* **89**, 468-483.

Frankel, A. D., D. L. Carver, and R. A. Williams (2002). Nonlinear and linear site response and basin effects in Seattle for the M 6.8 Nisqually, Washington earthquake, *Seism. Soc. Am. Bull.* **92**, 2090-2109.

Gower, H. D., J. C. Yount, and R. S. Crosson (1985). Seismotectonic map of the Puget Sound region, Washington, *U.S. Geol. Surv. Misc. Invest. Ser. Map* **I-1613,** scale 1:250,000.

Graves, R. W., A. Pitarka, and P. G. Somerville (1998). Ground-motion amplification in the Santa Monica area: Effects of shallow basin-edge structure, *Bull. Seism. Soc. Am.* **88**, 1224-1242.

Haugerud, R. A., D. J. Harding, S. Y. Johnson, J. L. Harless, C. S. Weaver, and B. L. Sherrod (2003). High-resolution lidar topography of the Puget Lowland, Washington-A bonanza for earth science, *GSA Today* **13**, 4-10.

Hiett, B. J. (2000). 3D geometry and velocity structure of the Tacoma basin, western Washington, *MS Thesis*, University of Texas at El Paso.

Hole, J. A. (1992). Nonlinear high-resolution three-dimensional seismic travel time tomography, *J. Geophys. Res.* **97**, 6553-6562.

Johnson, S. Y. (1984). Evidence for a margin-truncating transcurrent fault (pre-Late Eocene) in western Washington, *Geology* **12**, 538-541.

Johnson, S. Y. (1985). Eocene strike-slip faulting and nonmarine basin formation in Washington, in *Strike-Slip Deformation, Basin Formation, and Sedimentation*, edited by K.T. Biddle, and N. Christie-Blick, *Spec. Pub. Soc. Econ. Paleontol. Mineral.*, *37*, 283-302.

Johnson, S. Y., C. J. Potter, and J. M. Armentrout (1994). Origin and evolution of the Seattle fault and Seattle basin, Washington, *Geology* **22**, 71-74.

Johnson, S. Y., C. J. Potter, J. M. Armentrout, J. J. Miller, C. Finn, and C. S. Weaver (1996). The southern Whidbey Island fault: An active structure in the Puget Lowland, Washington, *Geol. Soc. Am. Bull.* **108**, 334-354.

Johnson, S. Y., S. V. Dadisman, J. R. Childs, and W. D. Stanley (1999). Active tectonics of the Seattle fault and central Puget Sound, Washington - Implications for earthquake hazards, *Geol. Soc. Am. Bull.* **111**, 1042-1053.

Johnson, S. Y., R. J. Blakely, W. J. Stephenson, S. V. Dadisman, and M. A. Fisher (2004). Active shortening of the Cascadia forearc and implications for seismic hazards of the Puget Lowland: *Tectonics*, 23, TC1011, doi:10.1029/2003TC001507, 27 pages.

Jones, M. A. (1996). Thickness of unconsolidated deposits in the Puget Sound Lowland, Washington and British Columbia, *U.S. Geol. Surv., Water Res. Invest Rept. (WRIR)* **94-4133**.

Jongmans, D., K. Pitilakis, D. Demanet, D. Raptakis, J. Riepl, C. Horrent, G. Tsokas, K. Lontzetidis,and P.-Y. Bard (1998). EURO-SEISTEST: Determination of the geological structure of the Volvi Basin and validation of the basin response, *Bull. Seism. Soc. Am.* **88**, 473-487.

Kawase, H. (1996). The cause of the damage belt in Kobe: "The basin-edge effect", constructive interference of the direct S wave with the basin-induced diffracted/Rayleigh waves, *Seism. Res. Lett.* **67**, 25-34.

Khazaradze, G., A. Qamar, and H. Dragert (1999). Tectonic deformation in western Washington from continuous GPS measurements, *Geophys. Res. Lett.* **26**, 3153-3156.

Li, Q., W. S. D. Wilcock, T. L. Pratt, C. M. Snelson, and T. M. Brocher (2004). Seismic attenuation structure of the Seattle basin, Washington State, from explosive-source refraction data, *Bull. Seism. Soc. Am.*, in review.

Miller, K. C., G. R. Keller, J. M. Gridley, J. H. Luetgert, W. D. Mooney and H. Thybo (1997). Crustal structure along the west flank of the Cascades, western Washington, *J. Geophys. Res.* **102**, 17,857-17,873.

Monger, J. W. H., and W. J. Nokleberg (1996). Evolution of the northern North American Cordillera: generation, fragmentation, displacement, and accretion of successive North American plate-margin arcs, in *Geology and ore deposits of the American Cordillera,* A. R. Coyner and P. L. Fahey (Eds.), Reno, NV, Geological Society of Nevada, 1133-1152.

Nelson, A. R., S. Y. Johnson, H. M. Kelsey, R. E. Wells, B. L. Sherrod, S. K. Pezzopane, L. A. Bradley, and R. D. Koehler, III (2003). Late Holocene earthquakes on the Toe Jam Hill fault, Seattle fault zone, Bainbridge Island, Washington, *Geol. Soc. Am. Bull.* **115**, 1388-1403.

Odum, J. K., W. J. Stephenson, K. Goetz-Troost, D. M. Worley, A. D. Frankel, R. A., Williams, and J. Fryer (2004). Shear- and compressional-wave velocity measurements from two 150-m-deep boreholes in Seattle, Washington, USA, *U.S. Geol. Surv. Open-File Rept.* **2004-1419**, 36 pp. http://pubs.usgs.gov/of/2004/1419/OF2004_1419.pdf.

Parsons, T., R. E. Wells, M. A. Fisher, E. Flueh, and U. S. ten Brink (1999). Three- dimensional

velocity structure of Siletzia and other accreted terranes in the Cascadia forearc of Washington, *J. Geophys. Res.* **104**, 18,015- 18,039.

Parsons, T., R. J. Blakely, and T. M. Brocher (2001). A simple algorithm for sequentially incorporating gravity observations in seismic traveltime tomography, *Intern. Geol. Rev.* **43**, 1073-1086.

Pratt, T. L., and T. M. Brocher (2004). Attenuation within sedimentary basins, and the shapes of site response estimates in the U.S. Pacific Northwest, *Bull. Seism. Soc. Am.*, in review.

Pratt, T. L., S. Johnson, C. Potter, W. Stephenson, and C. Finn (1997). Seismic reflection images beneath Puget Sound, western Washington state: The Puget Lowland thrust sheet hypothesis, *J. Geophys. Res.* **102**, 27,469-27,489.

Pratt, T. L., T. M. Brocher, C. S. Weaver, K. C. Miller, A. M. Tréhu, K. C. Creager, R. S. Crosson, and C. M. Snelson (2003a). Amplification of seismic waves by the Seattle basin, northwestern U.S., *Bull. Seism. Soc. Am.* **93**, 533-545.

Pratt, T. L., K. L. Meagher, T. M. Brocher, T. Yelin, R. Norris, L. Hultgrien, E. Barnett, and C. S. Weaver (2003b). Earthquake recordings from the 2002 Seattle Seismic Hazard Investigation of Puget Sound (SHIPS), Washington State, *U.S. Geol. Surv. Open-File Rept.* 03-361, 72 p. http://geopubs.wr.usgs.gov/open-file/of03-361/

Rau, W. W., and S. Y. Johnson (1999). Well stratigraphy and correlations, western Washington and northwestern Oregon, *U.S. Geol. Surv., Geo. Invest. Ser. Map* **I-2621**.

Riddihough, R. P. (1984). Recent movements of the Juan de Fuca plate system, *J. Geophys. Res.* **89**, 6980-6994.

Schuster, R. L., R. L. Logan and P. T. Pringle (1992). Prehistoric rock avalanches in the Olympic

Mountains, Washington, *Science* **258**, 1620-1621.

Sherrod, B. L., T. M. Brocher, C. S., Weaver, R. C. Bucknam, R. J. Blakely, H. M. Kelsey, A. R. Nelson, and R. Haugerud (2004). Holocene fault scarps near Tacoma, Washington, USA, *Geology* **32**, 9-12.

Snelson, C. M. (2001). Investigating crustal structure in western Washington and in the Rocky Mountains: Implications for seismic hazards and crustal growth, *Ph.D. Dissertation*, University of Texas at El Paso, 234 pp.

Tabor, J. J., and W. M. Cady (1978). The structure of the Olympic Mountains, Washington-analysis of a subduction zone, *U. S. Geol. Surv. Prof. Paper* **1033**, 38 pp.

ten Brink U. S., P. C. Molzer, M. A. Fisher, R. J. Blakely, R. C. Bucknam, T. Parsons, R. S. Crosson and K. C. Creager (2002). Subsurface geometry and evolution of the Seattle fault zone and the Seattle basin, Washington, *Bull. Seism. Soc. Am.* **92**, 1737-1753.

Van Wagoner, T. M., R. S. Crosson, K. C. Creager, G. F. Medema, L. A. Preston, N. P. Symons, and T. M. Brocher (2002). Crustal structure and relocated earthquakes in the Puget Lowland, Washington from high resolution seismic tomography, *J. Geophys. Re*s. **107**, ESE 22-1 to ESE 22-23, 10.10129/2001JB000710.

Wald, D. J. and R. W. Graves (1998). The seismic response of the Los Angeles basin, California, *Bull. Seism. Soc. Am.* **88**, 337-356.

Wells, D. L., and Coppersmith, K. J. (1994). New empirical relationships among magnitude, rupture length, rupture width, rupture area, and surface displacement, *Bull. Seism. Soc. Am*. **84**, 974-1002.

Wells, R. E., C. S. Weaver, and R. J. Blakely (1998). Fore-arc migration in Cascadia and its

neotectonic significance, *Geology* **26**, 759-762.

Zelt, C. A. (1998). Lateral velocity resolution from three-dimensional seismic refraction data, *Geophys. J. Int.* **135**, 1101-1112.

Department of Geoscience
University of Nevada Las Vegas
4505 Maryland Parkway, MS 4010
Las Vegas, Nevada 89154-4010
(C.M.S.)

U. S. Geological Survey
345 Middlefield Road, MS 977
Menlo Park, California 94025
(T.M.B.)

Department of Geological Sciences
University of Texas at El Paso
500 W. University Ave.
El Paso, Texas 79968
(K.C.M.)

U. S. Geological Survey
School of Oceanography
Box 357940
University of Washington
Seattle, Washington 98195
(T.L.P.)

College of Ocean and Atmospheric Sciences
Oregon State University
Corvallis, Oregon 97331
(A.M.T.)

Figures

Figure 1. A. Generalized geologic map of western Washington state (modified from Johnson et al., 1999). Seismic stations for "Dry" SHIPS are the small black dots and shot points are the small

stars. Abbreviations for cities: S - Seattle; T - Tacoma; O - Olympia; VI - Victoria. Circled 1, 2, and MK are stratigraphic column locations. Abbreviations for geologic features (fault - heavy lines, dashed where inferred; volcanoes – triangles): BH - Black Hills; CBF - Coast Range Boundary fault; DAF - Darrington fault; DF - Doty fault; DMF - Devils Mountain fault; GP - Glacier Peak; HC - Hood Canal fault; LRF - Leech River fault; MA - Mt. Adams; MB - Mt. Baker; MR - Mt. Rainer; MSH - Mt. St. Helens; SB - Seattle Basin; SCF - Straight Creek fault; SF - Seattle fault; SHZ - Saint Helens zone; SJ - San Juan Islands; SJF - San Juan fault; SWF - Southern Whidbey Island fault. B. Topographic base map of study area. Darker shades of gray represent higher elevations. 1999 SHIPS profile is indicated by gray dots (receiver stations) and stars (shotpoints). 2000 SHIPS is represented by a square. Major faults are indicated by dashed gray lines. Cities are in italics. Tomography model area is shown by the large dashed box. C. Stratigraphic column for the Puget Lowland. Shaded areas are intervals of non-deposition and/or erosion (modified from Johnson *et al.*, 1994; 1996).

Figure 2. Record from shot point 1 at the west end of the profile as seen. The Seattle basin is distinguished by a 2 s traveltime delay. The data are reduced at 6.5 km/s.

Figure 3. a. P-wave traveltime fits for the 1999 SHIPS data. Traveltimes are reduced at 6.5 km/s. Plus signs are the observed traveltimes, triangles are the calculated traveltimes from the inversion, and the dots are the residuals or difference between the observed and calculated traveltimes. b. S-wave traveltime fits for the 1999 SHIPS data. Traveltimes are reduced at 3.5 km/s. Plus signs are the observed traveltimes, triangles are the calculated traveltimes from the inversion, and the dots are the residuals or difference between the observed and calculated traveltimes.

Figure 4. a. Number of rays intersecting each cell for the 1999 SHIPS P-wave model. The minimum number of rays intersecting each cell is 5 and the maximum is 1884. b. Number of rays

intersecting each cell for the 1999 SHIPS S-wave model. The minimum number of rays intersecting each cell is 5 and the maximum is 420.

Figure 5. a. 15 km x 15 km recovered checkers along the 1999 SHIPS P-wave profile at 5% amplitude. b. 10 km x10 km recovered checkers along the 1999 SHIPS P-wave profile. c. 5 km x 5 km recovered checkers along the 1999 SHIPS P-wave profile.

Figure 6. A. 2-D velocity model derived from the final P-wave velocity model with a contour interval of 0.5 km/s. Shotpoints are signified by blue stars. Surface elevation is represented by a yellow line. The 4.5 km/s contour chosen as the base of the Seattle basin is highlighted in red. Major waterways along the profile are annotated. Yellow and black solid line segments represent the stratigraphy from ten Brink *et al.* (2002) where their profile crosses the Dry SHIPS profile. The dashed yellow lines and solid red line are an interpretation following the velocity contours where these beds would continue in our model. The thin vertical red lines at the top of the model are locations of postulated strike-slip faults with sense of motion (Johnson *et al.*, 1999). B. Enlarged portion of the 1999 SHIPS model with a contour interval of 0.2 km/s. The 3 sub-basins (SB) are labeled at the top. Abbreviations: Blakely Harbor Formation, Tbh; Blakeley Formation, Tb; Eocene, Eo; Crescent Formation, Cr.

Figure 7. Sonic logs for 5 industry boreholes located along the northern end of the Seattle basin, modified from Brocher *et al.* (2001). These wells did not intersect the Miocene Blakely Harbor Formation.

Figure 8. 1999 SHIPS P-wave velocity model overlaid with local seismicity with epicenters within 5 km of the profile. . The red lines are postulated strike-slip faults of Eocene age (Johnson *et al.*, 1999). A vertical band of seismicity in the upper 5 km of the Seattle basin near model km 70 coincides with the strike-slip faults and our proposed location for the Crescent/Cascade basement

contact. The band of seismicity represents a couple of earthquake swarms rather than a long-term seismic zone, but could indicate a basement fault extending into the sedimentary strata.

Figure 9. a. Amplification profiles from Pratt *et al,* (2003). b. Shear-wave model along the 1999 SHIPS profile with a contour interval of 0.25 km/s. Shotpoints are signified by blue stars. The red lines at the top of the model are locations of postulated strike-slip faults with sense of motion (Johnson *et al.*, 1999). The 3 sub-basins (SB) from Figure 6 are labeled at the top. Major faults and waterways along the profile are annotated.

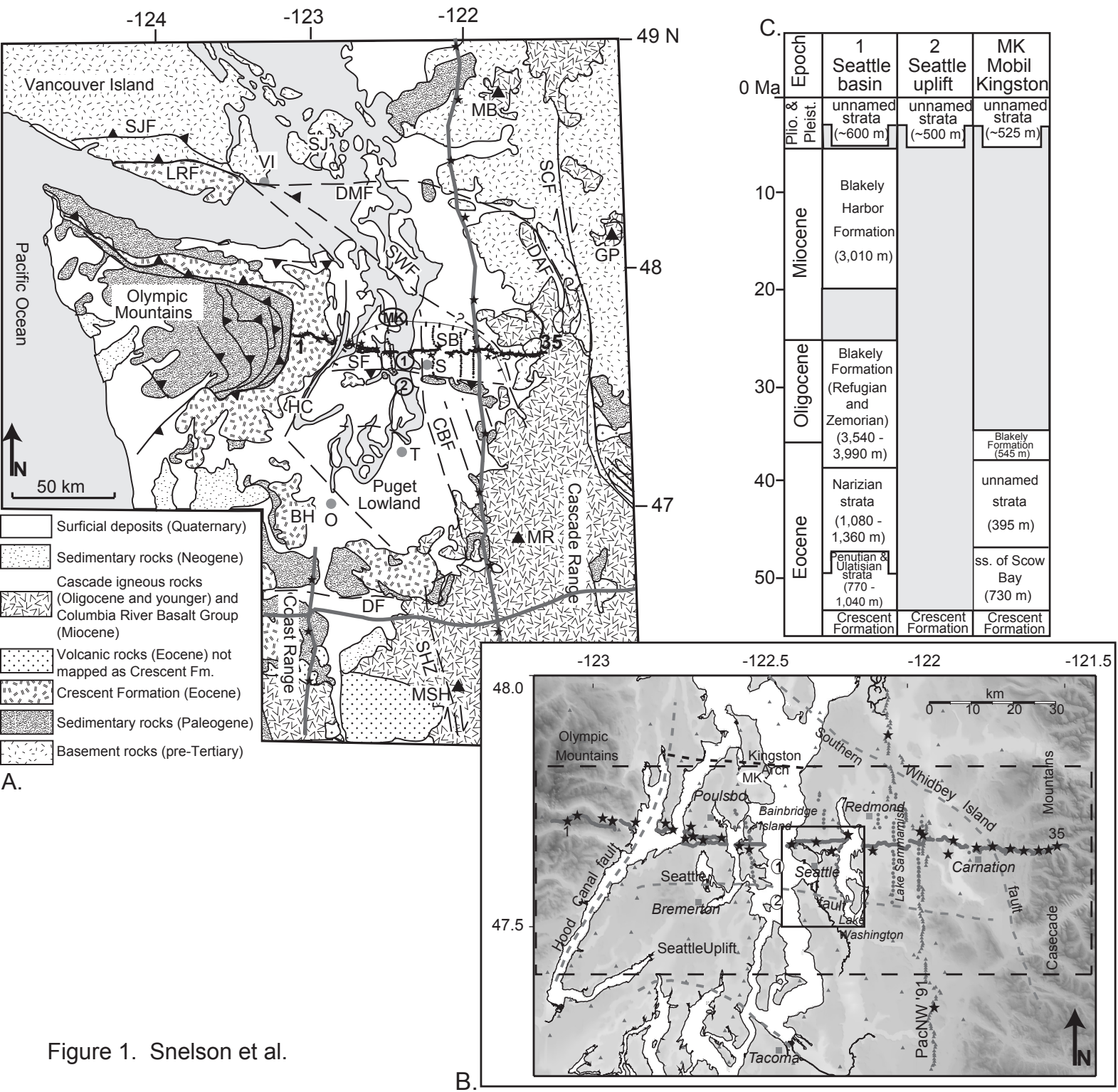

Figure 1. Snelson et al.

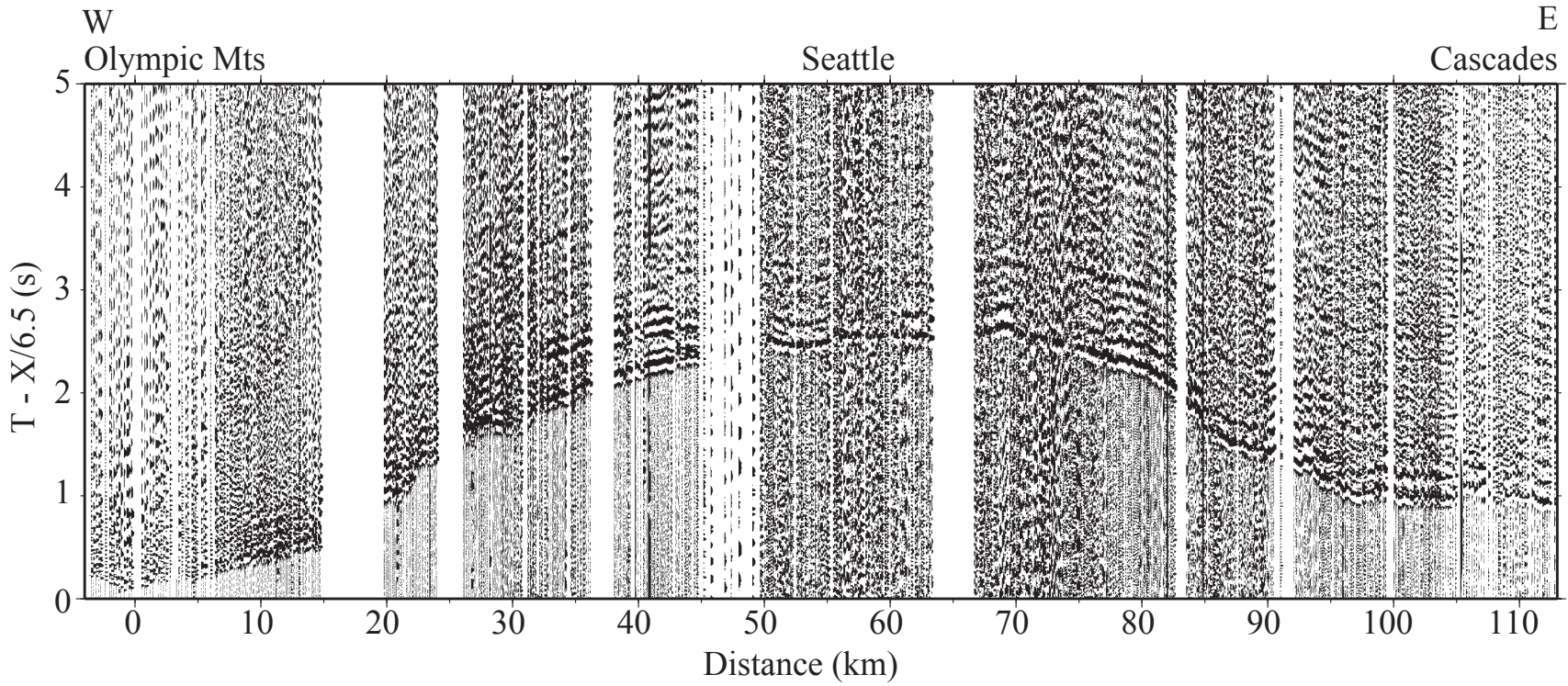

Figure 2. Snelson et al.

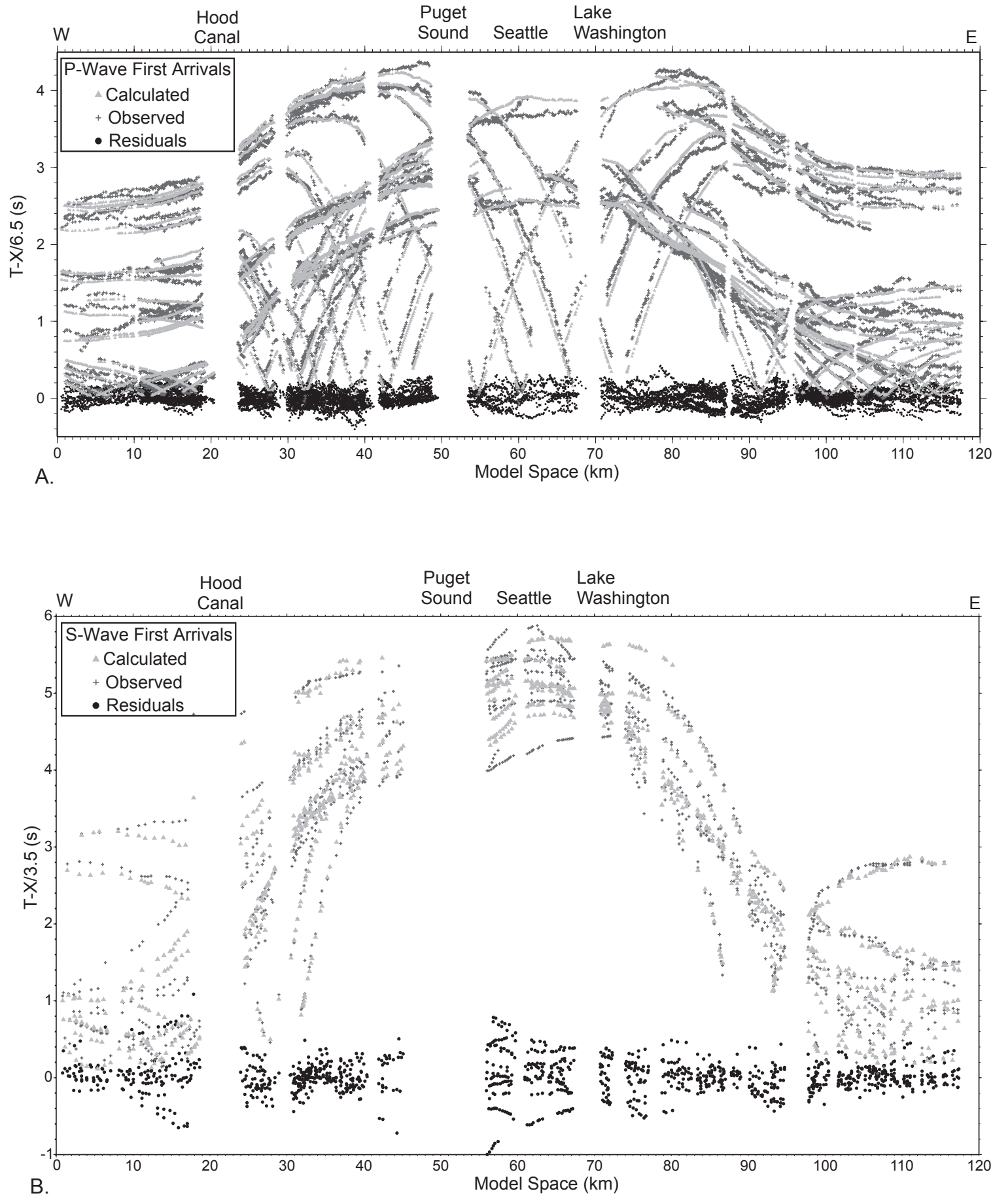

Figure 3. Snelson et al.

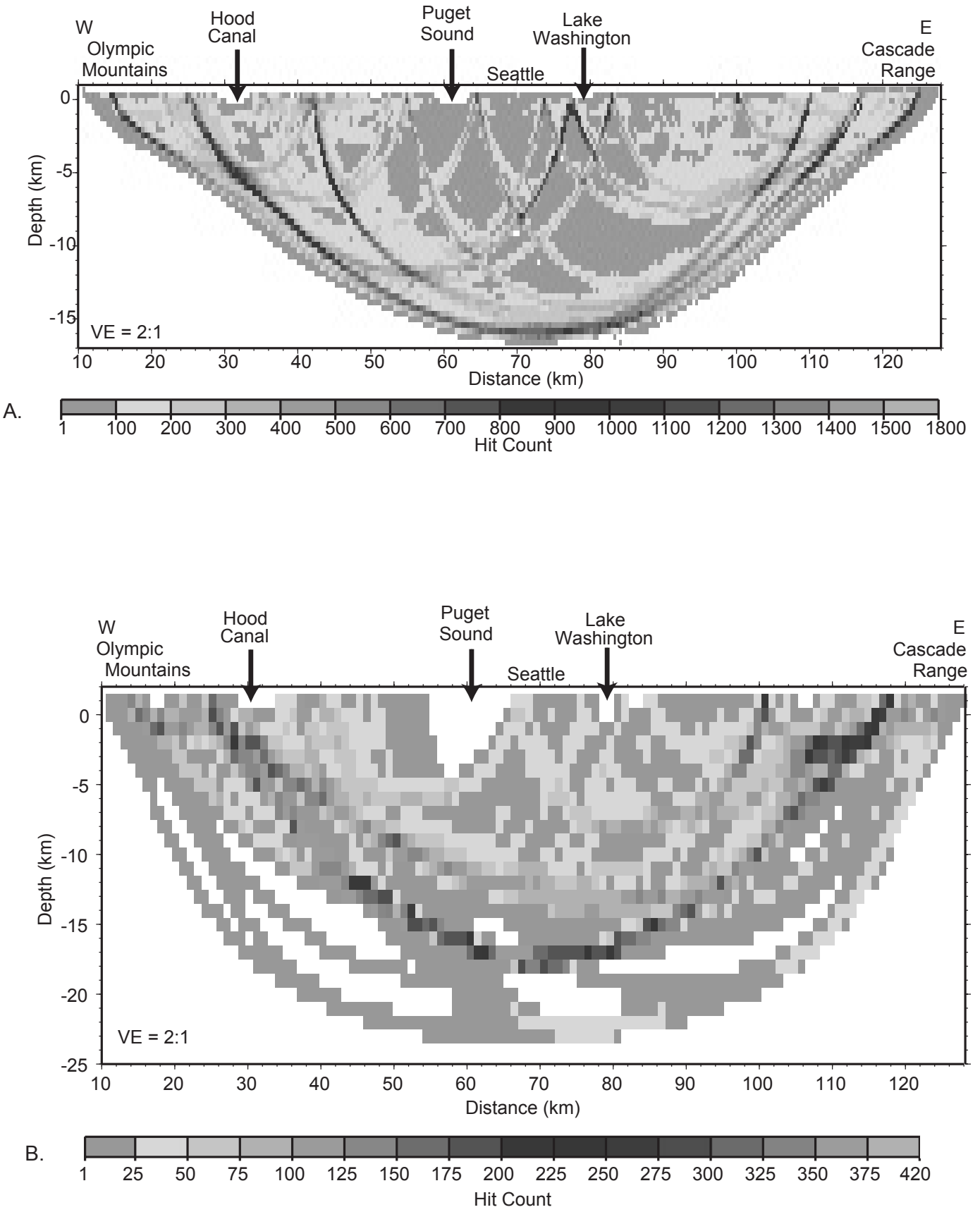

Figure 4. Snelson et al.

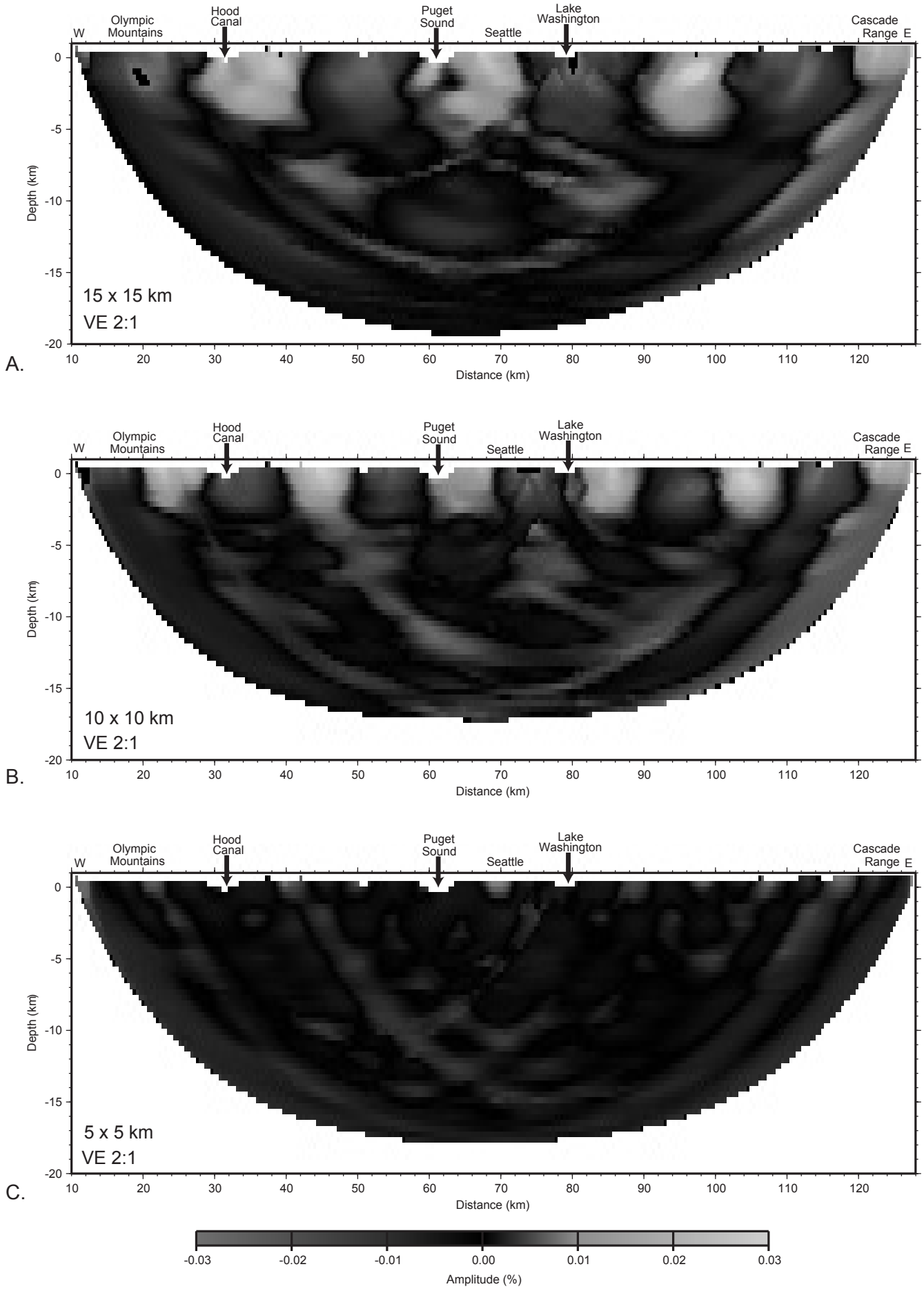

Figure 5. Snelson et al.

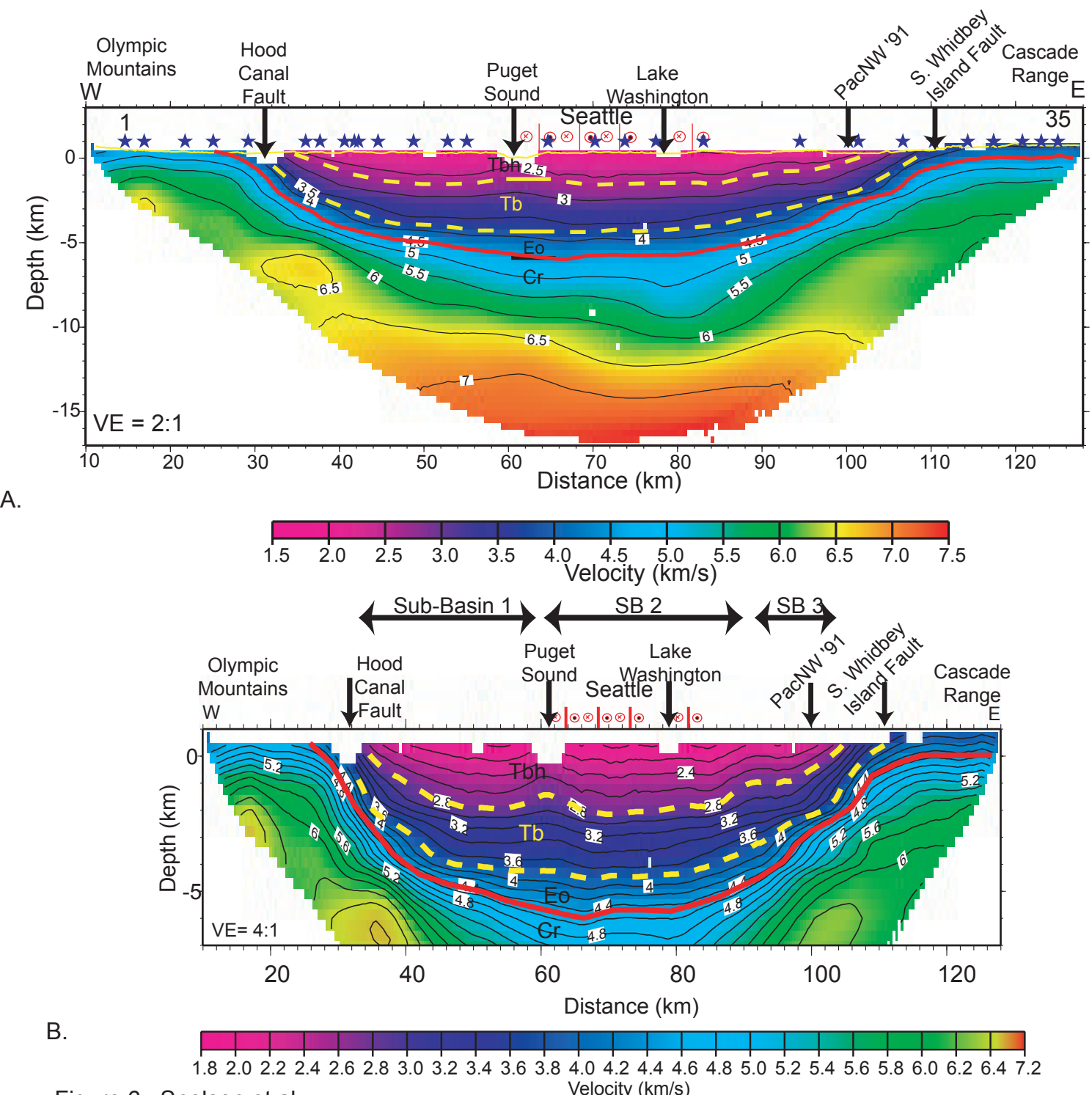

Figure 6. Snelson et al.

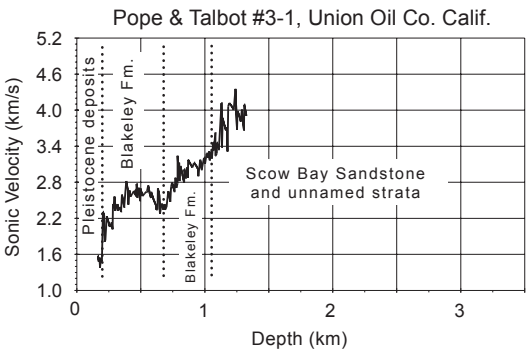

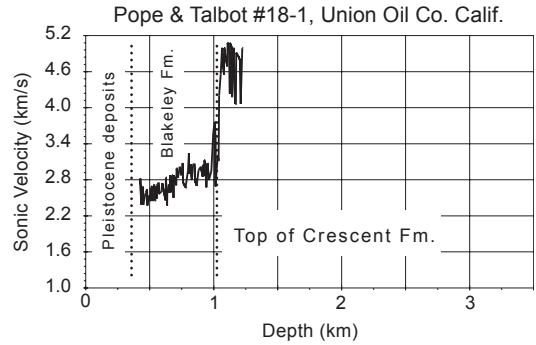

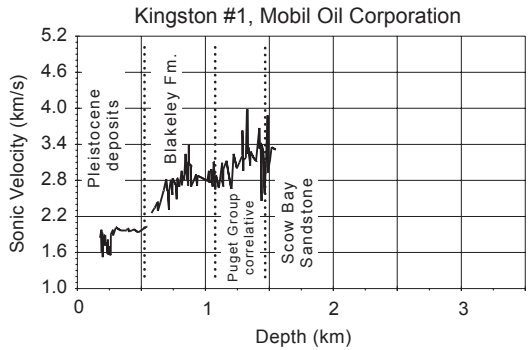

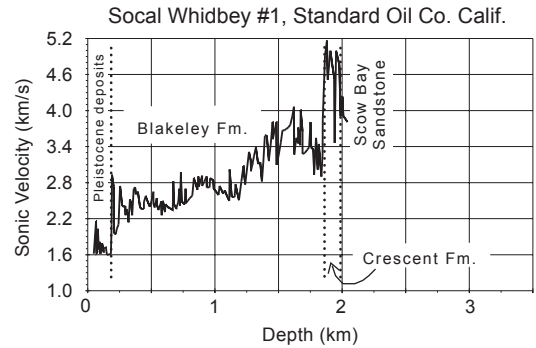

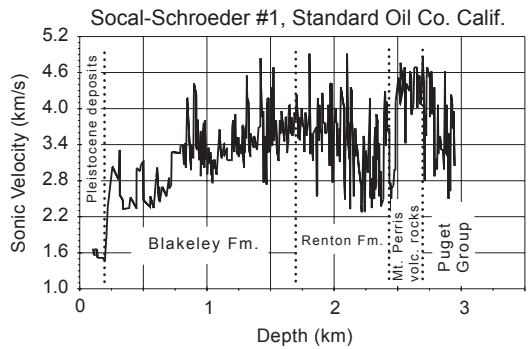

Figure 7. Snelson et al.

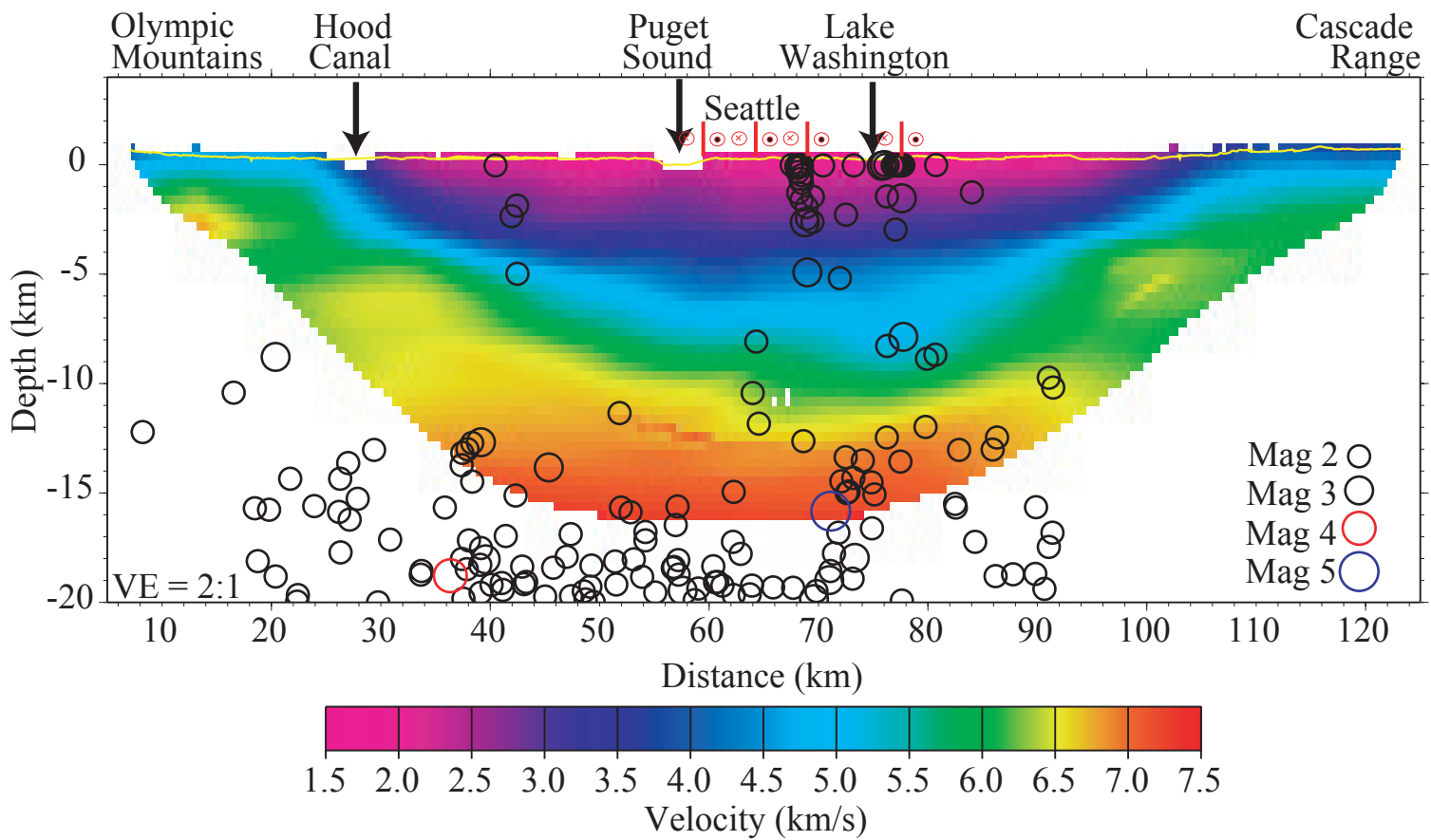

Figure 8. Snelson et al.

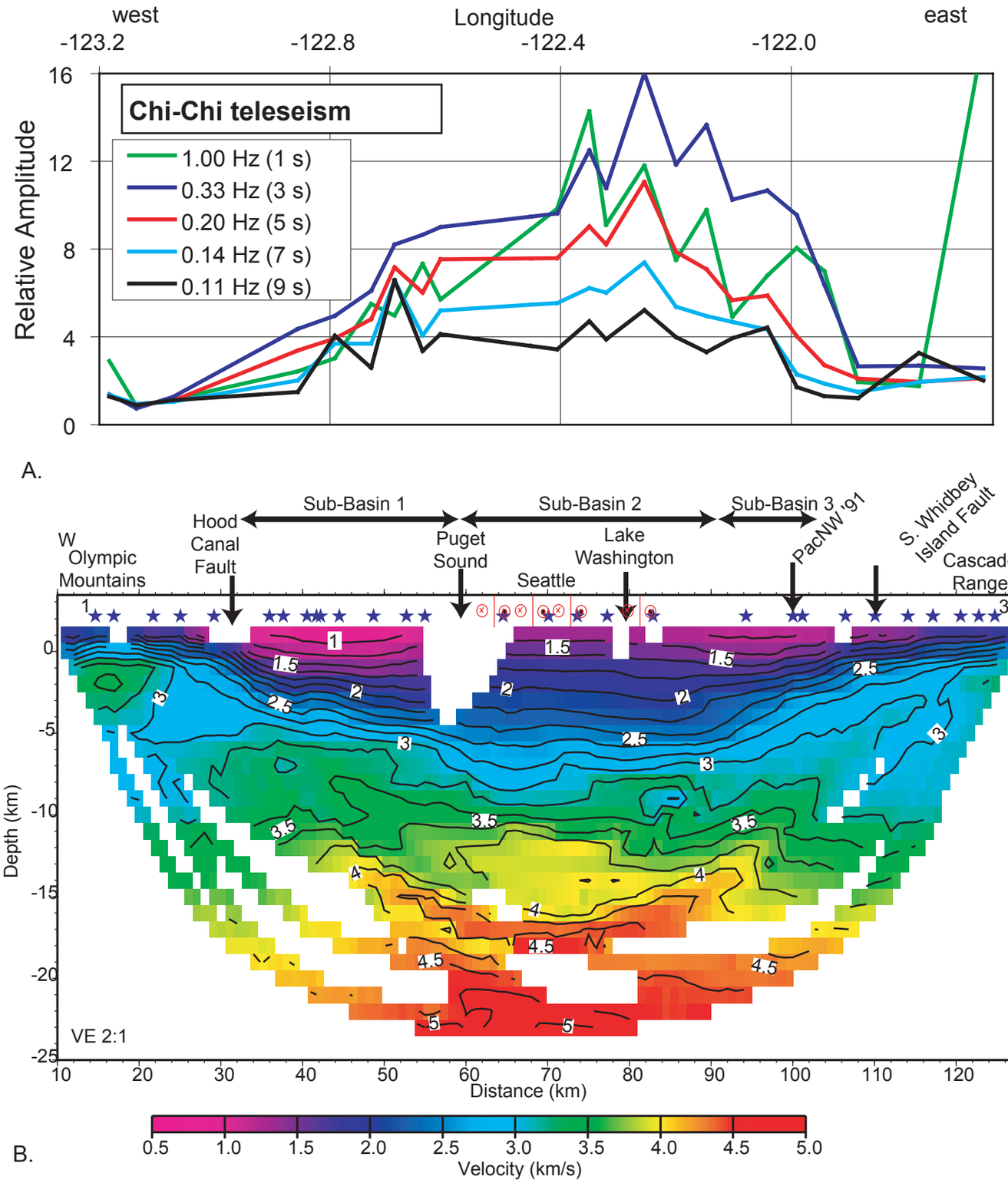

Figure 9. Snelson et al.